ENC-2022-0673
NUMERICAL STUDY OF FLOW PAST IN A ROTATING ELLIPTICAL CYLINDER FOR RE=5000

Mayara Francisca Reis de Souza
Augusto Salomão Bornschlegell
Fernando Augusto Alves Mendes

frsouza.mayara@gmail.com
augustosalomao@ufgd.edu.br
fernandomendes@ufgd.edu.br
Federal University of Grande Dourados - UFGD

Abstract. Using OpenFOAM software to carry out numerical simulations, it is possible to study a turbulent flow around a rotating elliptical cylinder with a fixed Reynolds number of 5000, varying the aspect ratio from 1 to 0.25. In simulations with the rotational elliptical cylinder in 2D, it is necessary to use a dynamic mesh, therefore, it is necessary to create a cell zone and baffles (to allow it to be possible to define the boundary conditions on the faces of the region) for the rotating zone, in order to have an Arbitrary Mesh Interface (AMI) allowing to define that the mesh represented by the rotating zone will be able to move freely and at the same time communicate with the rest of the domain. The chosen turbulence model is k-omega SST. The solver chosen was PIMPLE (pimpleFoam). The moment equations were solved using the second order upwind method (linearUpwindV grad(U)). For a temporal discretization of an implicit first order method, it was chosen (Euler). A changeable TimeStep was used to keep the Courant number below 0.5. The velocity ratio of the cylinder, what is in the range of 0 ≤ α ≤ 3, it induces a change in the distribution of pressure lines and at the point of stagnation, due to rotational movement in symmetrical bodies arises the lift force in also known as Magnus effect. In preliminary results it is possible to observe a periodic behavior, with maximum and minimum value for both lift force and drag force. Understanding this periodic phenomenon of the drag force and the lift force, study the values of relation cl / cd (lift coefficient divided by the drag coefficient) and knowing the influence of the velocity ratio in the cylinder aerodynamic forces is important in the feasibility analysis of the application of the Magnus effect in the engineering projects.

Keywords: Magnus Effect, Computational simulations, Re=5000, Rotating cylinder.

1. INTRODUCTION

It is common knowledge that conventional aerodynamic bodies have active forces present as shown in "Fig.1", disturbances can be easily observed by analyzing the streamlines that are formed by the flow.
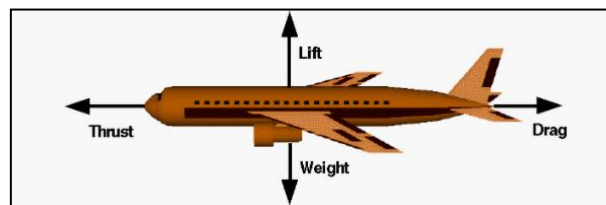

Figure 1. Aerodinamic forces – National Aeronautics and Space Administration.
Avaliable from: https://www.grc.nasa.gov/WWW/k-12/VirtualAero/BottleRocket/airplane/smotion.html

In flow, when the rotational velocity is added in a symmetrical body, it causes some regions of low and high pressure, which causes a change in the trajectory of a given body when it is immersed in a fluid. This is the Magnus Effect, a hydrodynamic phenomenon discovered by the scientist Heinrich Gustav Magnus (1802-1880), the first to study the effect

of lift on rotating bodies. We can clearly see in "Fig.2" how this phenomenon occurs, when the cylinder is rotating counterclockwise, the current lines in the region are compressed more aggressively than in the upper area, and in this way, it ends up generating a force of negative lift which is the objective of this numerical study.
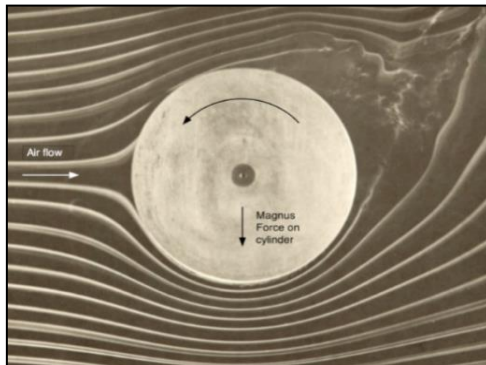

Figure 2. Streamlines from Magnus Effect – *Cross apud Brown (1971,1982)*
Avaliable from: http://www.physics.usyd.edu.au/~cross/TRAJECTORIES/Fluidflow%20Photos.pdf

The Magnus Effect is also present in sports such as tennis with a movement called slice, and has recently been used in wind turbine assemblies, as studied by "*Jinbo et al. (2016)*", which proved this improvement in the use of wind systems. In theory, the analysis of this type of experiment requires an apparatus with a certain complexity, such as the wind tunnel, with all the equipment to visualize the flow, which would have a high cost in terms of energy use in the purchase of equipment to improve the wind tunnel.

Some software is able to simulate the same flow, these are called CFD software (Computational Fluid Dynamics). The one used in this case was OpenFOAM ®, a widely used and free platform that makes possible the dynamics of interaction with graphical interfaces in order to facilitate the meshing process, and also the configuration of the simulation and the analysis of the results since the system it has an organization based on the system of files and folders as shown in "Fig.3".
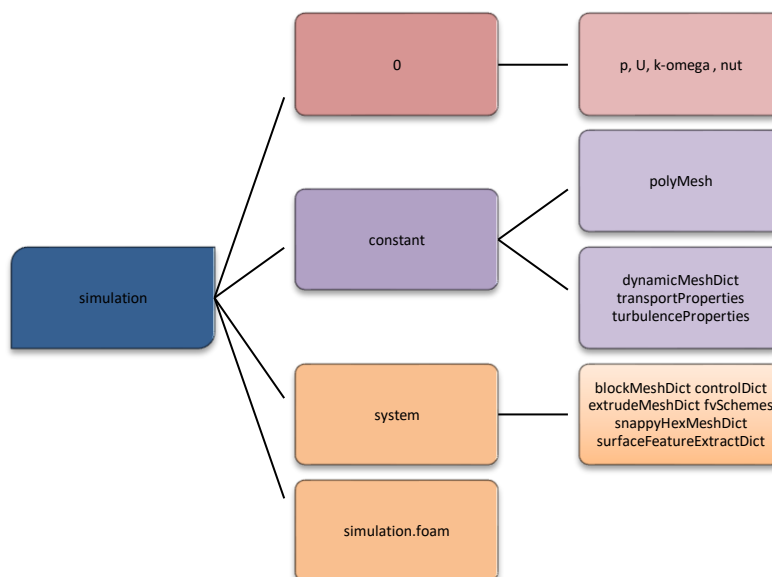

Figure 3. OpenFOAM ® system of files

2. MATHEMATICAL AND NUMRICAL MODELING

2.1 BOUNDARY CONDITIONS

The dimensional incompressible Navier–Stokes equations are employed as the governing equations. The Navier–Stokes final equations considering the coordinate direction $z = 0$ are as follows:

$$\frac{\partial u}{\partial t} + (u.\nabla).u = -\nabla\rho + \frac{1}{Re}\nabla.u \tag{1}$$

$$\nabla.u = 0 \tag{2}$$

So, in the "Eq. (1)", **u** represent the dimensionless velocity vector normalized by the velocity U_∞, t = t* U_∞/D, **p** is the dimensionless pressure normalized by ρU^2_∞, **Re** = U_∞*D/v is the Reynolds number, ρ is the fluid density, **D** is the diameter of the cylinder and **V** is the kinematic viscosity of the fluid. And the "Eq. (2)" represent the continuous equation simplified from the incompressible fluid.

For this simulation we use an Open-source Field Operation and Manipulation (OpenFOAM ®) ver8.0 software, the physics considerations were pre-defined and remain fixed for all simulations, as shown in "Tab.1" and "Tab.2". To carry out this work, five different simulations were performed where only the number of mesh cells was changed.

Table 1. Pre-defined physical considerations

Characteristic Length (m)	0.05
Reynolds number	5000
Kinematic air viscosity, sea level at 20°C	1.51E-05
Velocity ratio α	0.5
Specific weight of air, sea level at 20°C (kg/m^3)	1.225
Ambient air velocity at the fluid domain inlet (m/s)	1.562
Cylinder rotation velocity (rad/s) ω	1.208

Table 2. Simulation Parameter

Courant	0.5
Transient /incomprehensible	-
Solver	PimpleFoam
Velocity ratio $\alpha = \omega r/U\infty$	$0 \leq \alpha \leq 3$
Turbulence model	k-ω SST

Table 3. Boundary Conditions

Variables	Inlet	Outlet	Cylinder
k	0.06	zeroGradient	0
omega	0.0067	$internalField	$internalField
p	zeroGradient	fixedValue, uniform = 0	zeroGradient
U	1.562 m/s	0	0

The boundary conditions used in this simulation can be described in "Tab.3", where we can see specifically the adjustments of selected factors for the turbulence model k-omega SST and also for the pressure and velocity components. In the computational domain some areas have not changed for the variables *(p, k, omega and U)* and can be defined boundary condition as: Top and Bottom = symmetryPlane, Back and Front = empty, how is described in the "Fig.4".

When creating the geometry in OpenFOAM ®, the cylinder is in direct contact with the fluid and is in a turbulent regime rotating counterclockwise. The geometry can be checked in "Fig.4" and has dimensions 20Dx10Dx0.4D with the cylinder center located in 5D.
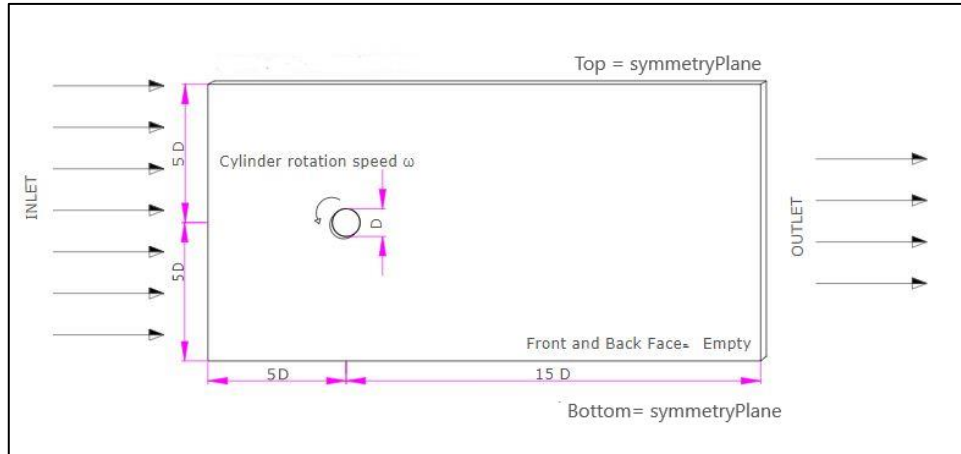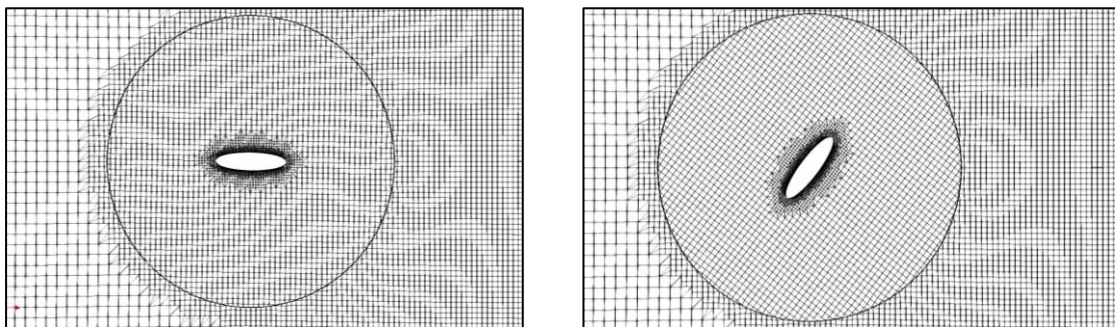
Figure 4. Computational Domain.

As the simulation is in two *2D* dimensions it is necessary to use *dynamicmesh* and after creating a cell-zone to be able to define the boundary conditions on the faces of the regions, in order to create the Arbitrary Mesh Interface (AMI) that allows the communication and movement of the rotating zone with the rest of the domain. The mesh settings used were based on the work of "*Lua, et al, 2018*". some of the specifications are present in "Tab.1". Being necessary to use the one-dimensional domain in the direction normal to the surface, in this way we designate "empty" for the back and front region.

As the results will be compared between five meshes with different refinements, after the settings in the *blockMeshDict* and *snappyHexMeshDict* files we need to proceed to the refinement in the area around the cylinder, where the distinction will be made between the number of cells and in the belt zone by accessing the *(AMI)* and granted permission to configure the rotating zone through *dynamicMeshDict*. As our geometry is being made in two dimensions, we have to access *snappyHexMeshDict*, which is used for refinement in 3D meshes, this results in a cell in the z direction, so the necessary readjustment can be done with the help of *extrudeMeshDict*.

## 2.3   MESH CARATERISTICS AND MATH

After this process of creating and refining the mesh using *extrudeMeshDict*, it is possible to visualize the surface using the ParaView® tool that illustrates the images of the computational domain as shown in "Fig.5". In (b) shows more closely the level of refinement of mesh, and it is observed that around the ellipse in the rotating zone the degree of refinement is greater than in the rest of the mesh, this derives from the concept that the more refined the mesh the more accurate are your results, (d) shows the mesh of the complete domain illustrated by the program
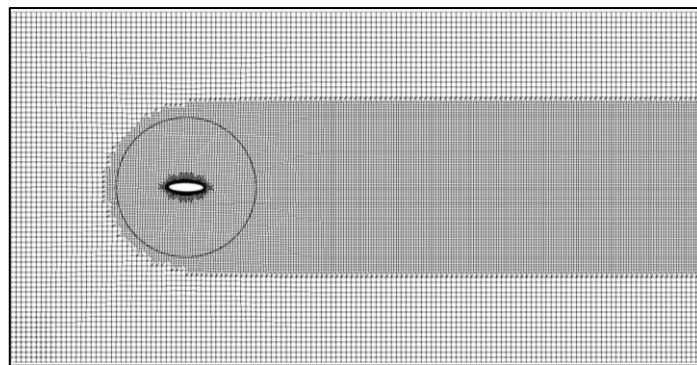

(a)   Faces of the cylinder
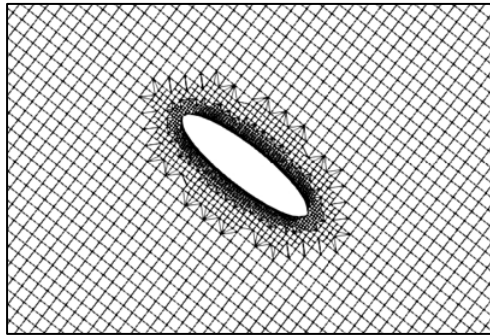
(b) Enlarged rotating zone
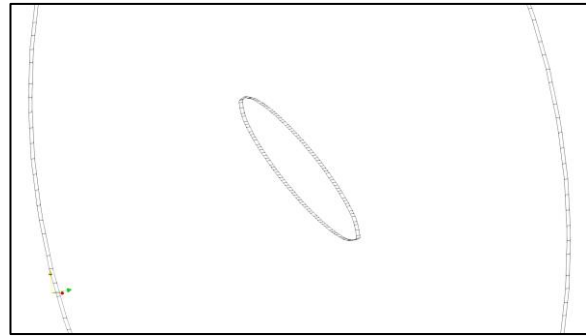
(c) Rotating zone without faces

(d) Mesh from the computational domain

Figure 5. Mesh illustration

After the meshes were refined, each one ended up showing some different characteristics, although some have the same total number of cells, the results obtained are slightly different due to the level of refinement of each mesh.

"Table 4" shows the geometric characteristics of the meshes as well as their order of refinement in ascending order starting with mesh I.

Table 4. Analysis of mesh geometry

Mesh	I	II	III	IV	V
Cells	12225	16889	16889	29247	29247
Hexahedral	11826	16397	16397	28607	28607
Prisms	108	136	136	176	176
Polyhedric	291	356	356	464	464

The turbulence model chosen was k-omega SST is a two-equation eddy-viscosity model which has become very popular, so the most suitable solver for the simulation is PimpleFoam, full descriptions to the "Eq. (5)" and "Eq. (6)" can be found on the *CFD-Online forum*. As previously mentioned, the variable TimeStep was defined and for a temporal discretization of an implicit first order method it was chosen (Euler), the initial mesh was based on the work of "*Lua, et al, (2018)*". As our objective is to analyze the cd/cl ratio for turbulent flow, the equations below are used to help the calculation:

The drag and lift coefficients have been defined by the equations:

$$C_L = \frac{F_D}{\rho U_\infty D} \tag{3}$$

$$C_D = \frac{F_L}{\rho U_\infty D} \tag{4}$$

The equation for the turbulence model k-omega SST is represent for:

$$\frac{\partial \omega}{\partial t} + U_j \frac{\partial \omega}{\partial x_j} = \propto S^2 - \beta \omega^2 + \frac{\partial \omega}{\partial x_j}\left[(v + \sigma_\omega vt)\frac{\partial \omega}{\partial x_j}\right] + 2(1 - F_1)\sigma_{\omega^2}\frac{1}{\omega}\frac{\partial k}{\partial x_i}\frac{\partial \omega}{\partial x_i} \tag{5}$$

$$\frac{\partial k}{\partial t} + U_j \frac{\partial k}{\partial x_j} = P_k - \beta * k\omega + U_j\frac{\partial}{\partial x_j}\left[v + \sigma_k vt)\frac{\partial k}{\partial x_j}\right] \tag{6}$$

3. RESULTS AND DISCUSSIONS

The following graphs in "Fig.6" more appropriately show the drag coefficients – cd and lift – cl, they are arranged in ascending order starting with the cl of mesh I, cd of mesh I and so on. It can be observed in the "Fig.7" that between the coefficients of mesh I to III there are some small changes, that is, the refinement of the mesh had an effect on the precision of the results, when we observe mesh IV, we see that the coefficients do not undergo any specific change mainly in the cd, this is due to the fact that for this study from mesh III onwards, the refinement level is not enough to change the mesh.
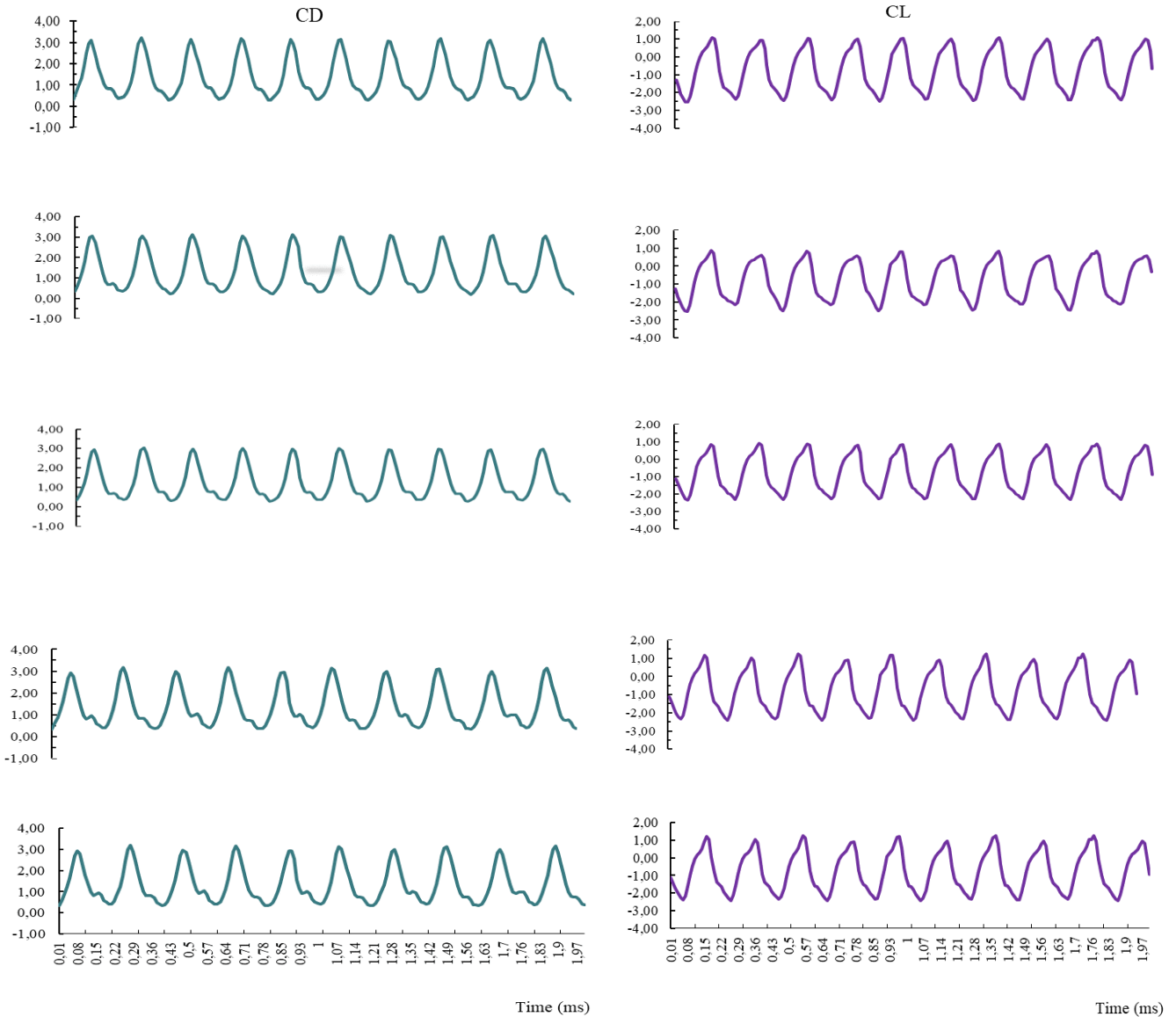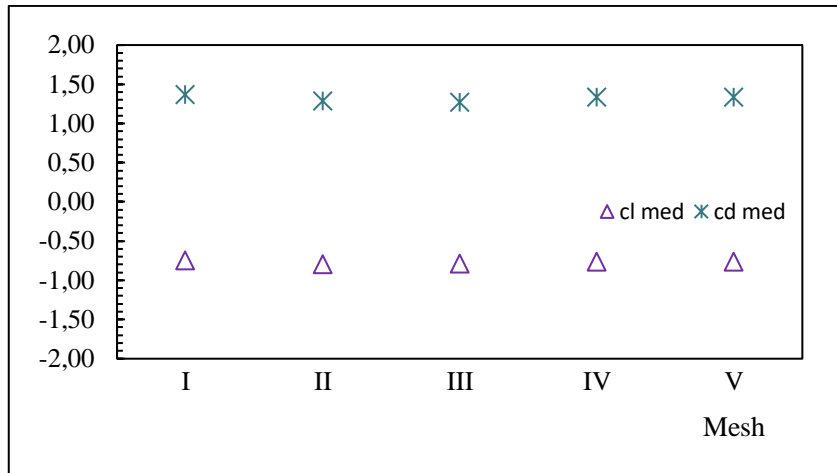

Figure 6. Results for cl and cd.

Figure 7. Medium value for the lift and drag force.

We can see in the "Fig.7" that the average coefficients have some peaks in relation to the others, this is because each mesh has a different level of refinement, which causes some variations in the results. However, when the mesh IV and V is observed, the results do not undergo practically any change, even with the flow in turbulent regime it still manages to remain stable and with some linear coefficients.
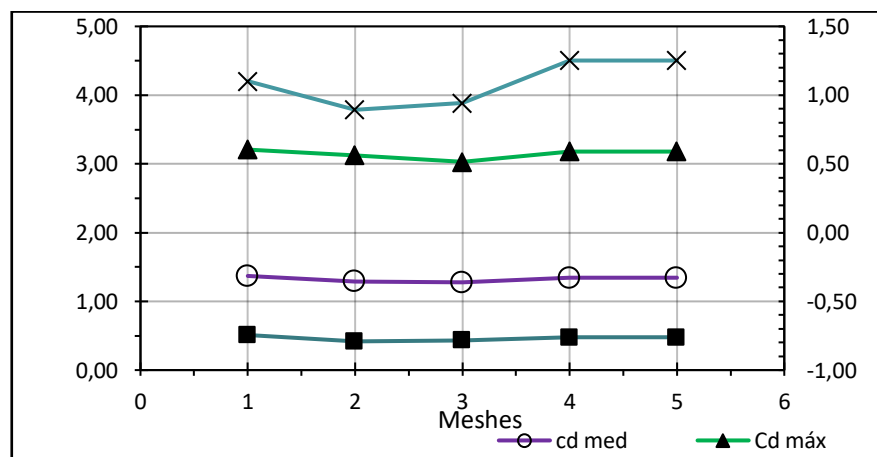

Figure 8. Relation forces cd/cl.

The graph of the relationship between cd/cl in "Fig.8" visually shows the average and maximum coefficients obtained for each mesh used in the flow in this simulation, we can observe that the cl max. has a growth peak from mesh III, and that the lift is always higher than the drag force, thus providing a good result for the simulation. In the relationship between the lift force and the drag force we see that the maximum lift remains greater than the drag, this shows that it was possible to validate the turbulent flow for the study of forces and the relationship to the average lift coefficient that increased atypically with increasing mesh refinement. The average lift value kept some negative values but as the cylinder is rotating counterclockwise this was to be expected.

From the data, we can also obtain images of the flow velocity field through the ParaView software, as mentioned above, and with it we can see the behavior of the vortices and how they behave over time, as shown in "Fig.9-11". In the cylinder, the vortex generation is continuous, but the pattern changes when the aspect ratio decreases during the interval of *(1 - 0.25)* it is this behavior that we see in the images obtained with ParaView where all velocity fields have $\alpha = 0.5$. The "Figure 9" we see that the motion of the vortices remains in a constant motion during the 2 s of the simulation in which the aspect ratio of the cylinder remains stable at a/b = 1, in "Fig.10" where the variation of the aspect ratio for a/b = 0.5 it is noticed that the pressure areas change and the vortices no longer remain with stable behavior, the same behavior is shown by the cylinder with the aspect ratio is a/b = 0.25 "Fig.11".

The distribution of pressure areas changes due to the aspect ratio variation, there is a pressure drop at the top of the cylinder and it increases linearly in relation to the aspect ratio decrease, so we can see that the lift in the cylinder increases depending on the angle at which it is located and that the effect of rotation causes it to suffer peaks and drops, showing the influences that the a/b ratio has on the flow.
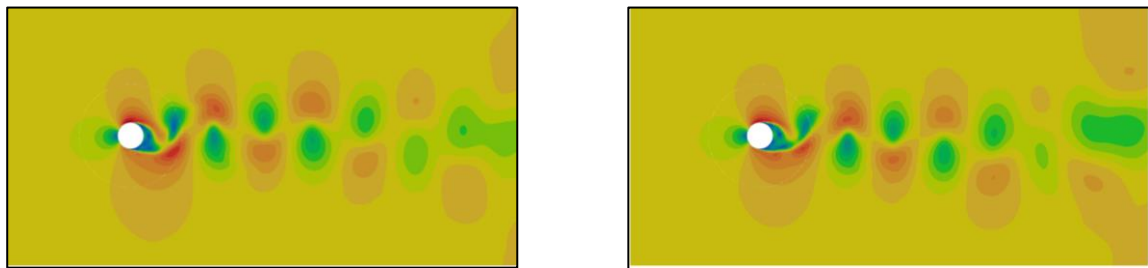
a)   Time: 1.3 s   (b) Time: 2 s

Figure 9. Velocity fields: α = 0.5, a/b = 1. (Autor 2022)
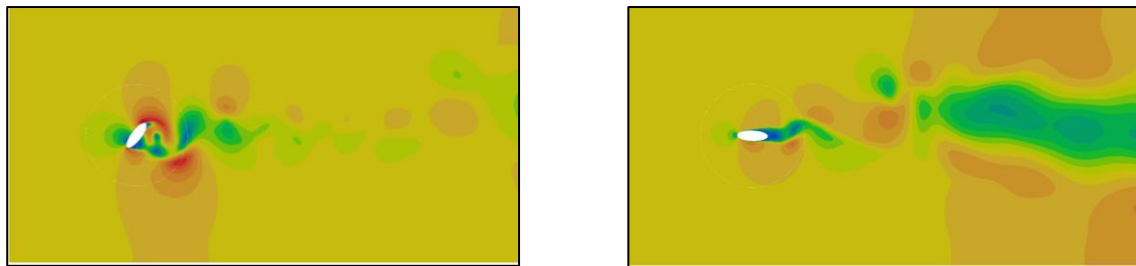
(c) Time: 1.3 s   (d) Time: 2 s

Figure 10. Velocity fields: α =0.5, a/b = 0.5. (Autor 2022)

(e) Time: 1.3 s   (f) Time: 2 s
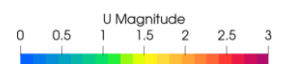
Figure 11. Velocity fields: α = 0.5, a/b = 0.25. (Autor 2022)

4. CONCLUSIONS

In this work, turbulent, incompressible and transient air flow is simulated inside a two-dimensional domain it is possible to observe that the level of mesh refinement directly influences the peak points obtained from the lift and drag coefficient, the results are satisfactory for the proposed study satisfactory because we can see an increase in lift and between the average values, despite the flow around a rotating cylinder being turbulent does not represent a great computational challenge, but the extreme refinement of a mesh do, in this way to improve the lift values it is necessary that the flow be more studied mainly the flow area where the refinement of the mesh is done.

We can this conclude that as the main objective is the validation of the use of the lift force, it is currently possible, although the refined mesh, at five different levels, has shown that the lift force has obtained a positive peak with values above the maximum drag we can see that the lift is stronger, even though the average is still lower it becomes negative due to the cylinder's rotation direction, validating the magnus effect in the simulation and making the results satisfactory.

As a recommendation for future work, perhaps a more extreme level of refinement in the mesh is necessary even if it requires a higher level of processing, according to *Quadros, R.C, (2018)*. the two-dimensional models may have some gaps in the analysis of results, so one would have to think also on various factors such as speed ratio and aspect ratio.

5. ACKNOWLEDGEMENTS

6. REFERENCES

CFD-ONLINE "SST k-omega model equations". Avaliable on: < https://www.cfd-online.com/Wiki/SST_k-omega_model>.

Jinbo, Maro; Cardoso Junior, Ghendy; Senter, Daniel; Santos, Edson Ribeiro dos; Farret, Felix Alberto, 2016; "*Turbina eólica de efeito Magnus: modelagem, protótipos e MPPT*", pp. 209-228. In Matemática aplicada à indústria: problemas e métodos de solução. São Paulo: Blucher,

Lua, K. B., Lu, H. e Lim, T. T., 2018. "Rotating Elliptic Cylinders in a Uniform Cross Flow", pp37-50. In Journal of Fluids and Structures. National Chiao Tung University, Taiwan.

Quadros, R.C, 2018. "Simulação Numérica de Modelos de Turbulência para o Efeito Magnus", Tese de dissertação UTFPR. < https://educapes.capes.gov.br/handle/1884/58423>.

7. RESPONSIBILITY NOTICE

The authors are the only responsible for the printed material included in this paper.